*Inorg. Chem.* **2004**, *43*, 3098–3105


# Proton Transfer to Nickel–Thiolate Complexes. 1. Protonation of $[Ni(SC_6H_4R\text{-}4)_2(Ph_2PCH_2CH_2PPh_2)]$ (R = Me, MeO, H, Cl, or $NO_2$)

**Valerie Autissier, William Clegg, Ross W. Harrington, and Richard A. Henderson***

*Chemistry, School of Natural Sciences, University of Newcastle, Newcastle upon Tyne, NE1 7RU U.K.*

Received November 14, 2003

The kinetics of the equilibrium reaction between $[Ni(SC_6H_4R\text{-}4)_2(dppe)]$ (R= MeO, Me, H, Cl, or $NO_2$; dppe = $Ph_2PCH_2CH_2PPh_2$) and mixtures of $[lutH]^+$ and lut (lut = 2,6-dimethylpyridine) in MeCN to form $[Ni(SHC_6H_4R\text{-}4)(SC_6H_4R\text{-}4)(dppe)]^+$ have been studied using stopped-flow spectrophotometry. The kinetics for the reactions with R = MeO, Me, H, or Cl are consistent with a single-step equilibrium reaction. Investigation of the temperature dependence of the reactions shows that $\Delta G^{\ddagger} = 13.6 \pm 0.3$ kcal mol$^{-1}$ for all the derivatives but the values of $\Delta H^{\ddagger}$ and $\Delta S^{\ddagger}$ vary with R (R = MeO, $\Delta H^{\ddagger} = 8.5$ kcal mol$^{-1}$, $\Delta S^{\ddagger} = -16$ cal K$^{-1}$ mol$^{-1}$; R = Me, $\Delta H^{\ddagger} = 10.8$ kcal mol$^{-1}$, $\Delta S^{\ddagger} = -9.5$ cal K$^{-1}$ mol$^{-1}$; R = Cl, $\Delta H^{\ddagger} = 23.7$ kcal mol$^{-1}$, $\Delta S^{\ddagger} = +33$ cal K$^{-1}$ mol$^{-1}$). With $[Ni(SC_6H_4\text{-}NO_2\text{-}4)_2(dppe)]$ a more complicated rate law is observed consistent with a mechanism in which initial hydrogen-bonding of $[lutH]^+$ to the complex precedes intramolecular proton transfer. It seems likely that all the derivatives operate by this mechanism, but only with R = $NO_2$ (the most electron-withdrawing substituent) does the intramolecular proton transfer step become sufficiently slow to result in the change in kinetics. Studies with $[lutD]^+$ show that the rates of proton transfer to $[Ni(SC_6H_4R\text{-}4)_2(dppe)]$ (R = Me or Cl) are associated with negligible kinetic isotope effect. The possible reasons for this are discussed. The rates of proton transfer to $[Ni(SC_6H_4R\text{-}4)_2(dppe)]$ vary with the 4-R-substituent, and the Hammett plot is markedly nonlinear. This unusual behavior is attributable to the electronic influence of R which affects the electron density at the sulfur.

## Introduction

Understanding the factors which control the rates and mechanisms of protonation of metal complexes is fundamental in defining the elementary reactions both of certain metalloenzymes, including nitrogenases and hydrogenases,[1,2] and of certain industrially and economically important catalysts, such as those involved in the isomerization or hydrocyanation of alkenes and alkynes.[3,4] Previous kinetic studies have revealed that apparently simple protonation reactions of transition metal complexes can be mechanistically complicated, because protonation can occur at more than one site in these complexes: either metal or ligand.[5,6] In many complexes rapid protonation at one site (kinetically favored protonation site) is followed by intra- or intermolecular rearrangements in which the proton "moves" to another site (thermodynamically favored protonation site) to give the product. Much of this chemistry has been defined with complexes containing metal−carbon bonds, where the rates of protonation of both the metal and carbon sites are appreciably slower than the diffusion-controlled limit ($k_{diff} = 1 \times 10^{10}$ dm$^3$ mol$^{-1}$ s$^{-1}$).[7] It is generally accepted that proton transfer at carbon sites is slow because of the change in hybridization of the carbon, and proton transfer at metal sites is slow because of the changes in the coordination geometry and the diffuse nature of the electron density at a metal (i.e., no stereochemical lone pair of electrons).[8]

* To whom correspondence should be addressed. E-mail: r.a.henderson@ncl.ac.uk.

(1) (a) Henderson, R. A. *Nitrogen Fixation at the Millenium*; Leigh, G. J., Ed.; Elsevier: Amsterdam, 2002; Chapter 9. (b) Burgess, B. K.; Lowe, D. J. *Chem. Rev.* **1996**, *96*, 2983.
(2) (a) Henderson, R. A. *Recent Advances in Hydride Chemistry*; Peruzzini, M., Poli, R., Eds.; Elsevier: Amsterdam, 2001; Chapter 16. (b) Cammack, R.; Vliet, P. *Bioinorganic Catalysis*, 2nd ed.; Reedijk, J., Bouwmann, E., Eds.; Marcel Dekker: New York, 1999; Chapter 9. (c) Henderson, R. A. *J. Chem. Res., Synop.* **2002**, 407.
(3) Masters, C. *Homogeneous Transition Metal Chemistry*; Chapman and Hall: London, 1981; pp 135−158.
(4) Jolly, P. W.; Wilke, G. *Organic Chemistry of Nickel*; Academic Press: New York, 1975; Vol. 2, Chapter 5.
(5) (a) Kramarz, K. W.; Norton, J. R. *Prog. Inorg. Chem.* **1994**, *42*, 1. (b) Kristjansdottir, S. S.; Norton, J. R. *Transition Metal Hydrides: Recent Advances in Theory and Experiment*; Dedieu, A., Ed.; VCH: New York, 1992; Chapter 9.
(6) Henderson, R. A. *Angew. Chem., Int. Ed. Engl.* **1996**, *35*, 946.
(7) Eigen, M. *Angew. Chem., Int. Ed. Engl.* **1964**, *3*, 1.



10.1021/ic030322e CCC: $27.50 
Published on Web 04/20/2004

It might be anticipated that proton transfer to transition metal complexes containing ligands with group 16 or 17 donor atoms would be less complicated than protonation of organometallic complexes. In general, protonation of stereochemical lone pairs of electrons on group 16 or 17 atoms in ligands is diffusion-controlled, and is much faster than the rate of protonation of the metal. In addition, group 16 or 17 donor atoms are often markedly more basic than the metal. Thus, protonation of such ligands is favored (both kinetically and thermodynamically) over protonation of the metal.

Using the few general principles outlined above, it is possible to predict the rates of proton transfer in a variety of different metal complexes. However, some exceptions to the general patterns are emerging. We have been particularly interested in the rates of proton transfer to sulfur sites in compounds which mimic active sites of metalloenzymes. Thus, we have established that protonation of synthetic Fe−S-based clusters which contain dimeric $\{MFe(\mu\text{-}S)_2\}^{2+}$ or cuboidal $\{MFe_3(\mu_3\text{-}S)_4\}^{n+}$ (M = Fe, Mo or W) cores is an entirely general phenomenon.[9] Protonation has been attributed to reactions of the $\mu_n$-S sites, and the p$K_a$'s of the protonated clusters are essentially independent of the topology, charge, nuclearity, or terminal ligands on the clusters (p$K_a$ = 18.4 ± 0.5).[10] More recently, the rates of protonation of these clusters have been shown to be slower than the diffusion-controlled limit and are markedly dependent on the metal composition of the cluster.[11]

Thiolate sulfur (cysteinate) is a ligation common in bioinorganic chemistry, and protonation of such ligands is a reaction which is invoked in the reactions of many metalloenzymes, most notably nitrogenases,[12] hydrogenases,[13] and Fe−S-based hydrolases such as aconitase.[14] Little is known about the protonation of simple coordinated thiolates. It is generally assumed that the reactions are diffusion-controlled. However, some recent studies by us have indicated that proton transfer reactions involving simple transition metal thiolates are, at least in certain cases, slow.[15]

In this paper, we report studies on the protonation reactions of $[Ni(SC_6H_4R\text{-}4)_2(dppe)]$ (R = MeO, Me, H, Cl, or $NO_2$; dppe = $Ph_2PCH_2CH_2PPh_2$) with $[lutH]^+$ (lut = 2,6-dimethylpyridine) in MeCN and show that protonation of the thiolate sulfur is typified by the following observations: (i) proton transfer is slow; (ii) the metal effectively "levels" the acidity of the coordinated thiol; and (iii) with most derivatives the kinetics are simple, but when R = $NO_2$ a more complicated rate law is observed, consistent with a mechanism involving rapid formation of a hydrogen-bonded precursor prior to rate-limiting intramolecular proton transfer. In the following paper[16] we elaborate further on the mechanistic aspects of proton transfer to nickel thiolate complexes by studies on $[Ni(SC_6H_4R\text{-}4)(triphos)]^+$ {triphos = $PhP(CH_2CH_2PPh_2)_2$}. In this class of complexes, the kinetics of the protonation reactions of all derivatives are consistent with a mechanism in which a hydrogen-bonded adduct between the acid and complex can be detected prior to the rate-limiting intramolecular proton transfer to form $[Ni(SHC_6H_4R\text{-}4)(triphos)]^{2+}$. Studies on $[Ni(SC_6H_4R\text{-}4)(triphos)]^+$ allow the kinetic characterization of intramolecular proton transfer reactions.

**Table 1.** Analysis and Spectroscopic Characteristics of $[Ni(SC_6H_4R\text{-}4)_2(dppe)]^+$ (R = $NO_2$, Cl, H, Me, or MeO; dppe = $Ph_2PCH_2CH_2PPh_2$)

| | elemental analysis/%[a] | | | NMR spectroscopy | |
|---|---|---|---|---|---|
| R | C | H | N | $^1H$[b,c] | $^{31}P$[d] |
| $NO_2$ | 59.80 (59.96) | 4.19 (4.18) | 3.68 (3.67) | | 56.95 |
| Cl | 61.14 (61.29) | 4.18 (4.30) | | | 57.38 |
| H | 66.63 (67.55) | 4.83 (5.04) | | | 56.50 |
| Me | 68.15 (68.27) | 5.23 (5.40) | | 2.1 (Me) | 56.40 |
| MeO | 65.35 (65.31) | 5.16 (5.17) | | 5.7 (MeO) | 55.70 |

[a] Calculated values shown in parentheses. [b] Chemical shifts relative to TMS. [c] Peaks due to dppe ligands are present in all spectra at $\delta$ 7.0−8.0 (multiplets, Ph groups) and $\delta$ 2.2−3.0 (doublet, $CH_2$); peaks due to 4-$RC_6H_4S$ are present in all spectra at $\delta$ 6.0−7.0 (multiplets). [d] Chemical shifts relative to $H_3PO_4$, singlets.

## Experimental Section

All preparations and manipulations were routinely performed under an atmosphere of dinitrogen using Schlenk or syringe techniques as appropriate. All solvents were dried and freshly distilled from the appropriate drying agent immediately prior to use.

The thiols 4-$RC_6H_4SH$ (R = $NO_2$, Cl, Me, or MeO), lut (lut = 2,6-dimethylpyridine), and $Ph_2PCH_2CH_2PPh_2$ (dppe) were purchased from Aldrich and used as received. $NaSC_6H_4R\text{-}4$,[17] $[lutH]BPh_4$,[18] and $[lutD]BPh_4$ were prepared by literature methods. $[NiCl_2(dppe)]$ was prepared by the method reported earlier.[19]

**Preparation of $[Ni(SC_6H_4R\text{-}4)_2(dppe)]$ (R = $NO_2$, Cl, H, Me, or MeO).** The complexes in the series $[Ni(SC_6H_4R\text{-}4)_2(dppe)]$ were all prepared by the same method.[20] The complexes were characterized by elemental and spectroscopic analysis as shown in Table 1, and (for R = H, Cl, or Me) by X-ray crystallography. A typical preparation is described below for $[Ni(SC_6H_4Me\text{-}4)_2(dppe)]$.

To a suspension of $[NiCl_2(dppe)]$ (1 g, 1.95 mmol) in ethanol (ca. 30 mL) was added an excess of $NaSC_6H_4R\text{-}4$ (6.0 mmol). The


(8) Bell, R. P. *The Proton in Chemistry*, 2nd ed.; Chapman and Hall: London, 1973; Chapter 10 and references therein.
(9) (a) Henderson, R. A.; Oglieve, K. E. *Chem. Commun*. **1994**, 377. (b) Almeida, V. R.; Gormal, C. A.; Grönberg, K. L. C.; Henderson, R. A.; Oglieve, K. E.; Smith, B. E. *Inorg. Chim. Acta* **1999**, *291*, 212. (c) Henderson, R. A.; Oglieve, K. E. *J. Chem. Soc., Dalton Trans*. **1998**, 1731.
(10) Grönberg, K. L. C.; Henderson, R. A. *J. Chem. Soc., Dalton Trans*. **1996**, 3667.
(11) (a) Henderson, R. A.; Oglieve, K. E. *J. Chem. Soc., Dalton Trans*. **1999**, 3927. (b) Henderson, R. A.; Dunford, A. J. *Chem. Commun*. **2002**, 360. (c) Bell, J.; Dunford, A. J.; Hollis, E.; Henderson, R. A. *Angew. Chem.* **2003**, *42*, 1149.
(12) Burgess, B. K.; Lowe, D. *J. Chem. Rev.* **1996**, *96*, 2983.
(13) Peters, J. W.; Lanzilotta, W. N.; Lemon, B. J.; Seefeldt, L. C. *Science* **1998**, *282*, 1853
(14) Flint, D. H.; Allen, R. M. *Chem. Rev.* **1996**, *96*, 2315.
(15) Clegg, W.; Henderson, R. A. *Inorg. Chem.* **2002**, *41*, 1128.
(16) Accompanying paper: Autissier, V.; Zarza, P. M.; Petrou, A.; Henderson, R. A.; Harrington, R. W.; Clegg, W. *Inorg. Chem.* **2004**, *43*, 3106−3115.
(17) Hagen, K. S.; Holm, R. H. *Inorg. Chem*. **1984**, *23*, 418.
(18) Grönberg, K. L. C.; Henderson, R. A.; Oglieve, K. E. *J. Chem. Soc., Dalton Trans*. **1998**, 3093.
(19) Busby, R.; Hursthouse, M. B.; Jarrett, P. S.; Lehmann, C. W.; Abdul Malik, K. M.; Phillips, C. *J. Chem. Soc., Dalton Trans.* **1993**, 3767.
(20) Hayter, R. G.; Humiec, F. S. *J. Inorg. Nucl. Chem*. **1964**, *26*, 807.

**Table 2.** Crystal Data and Structure Refinement Parameters for $[Ni(SC_6H_4R\text{-}4)_2(dppe)]$ (R = H, Me, or Cl; dppe = $Ph_2PCH_2CH_2PPh_2$)

| | $[Ni(SC_6H_5)_2(dppe)]$ | $[Ni(SC_6H_4\text{-}Me\text{-}4)_2(dppe)]$ | $[Ni(SC_6H_4Cl\text{-}4)_2(dppe)]\cdot 0.25CH_2Cl_2$ |
|---|---|---|---|
| formula | $C_{38}H_{34}NiP_2S_2$ | $C_{40}H_{38}NiP_2S_2$ | $C_{38}H_{32}Cl_2NiP_2S_2\cdot 0.25CH_2Cl_2$ |
| fw | 675.42 | 703.47 | 765.53 |
| cryst syst | monoclinic | monoclinic | triclinic |
| space group | $C2/c$ | $P2_1/n$ | $P\bar{1}$ |
| $T$, K | 150 | 150 | 150 |
| $a$, Å | 14.3764(16) | 11.4276(6) | 13.6352(7) |
| $b$, Å | 15.9241(12) | 17.6539(9) | 16.5127(8) |
| $c$, Å | 14.1357(13) | 17.2914(8) | 18.9762(10) |
| $\alpha$, deg | | | 65.255(1) |
| $\beta$, deg | 92.756(2) | 100.337(1) | 75.748(1) |
| $\gamma$, deg | | | 71.427(1) |
| $V$, Å$^3$ | 3232.4(5) | 3431.8(3) | 3646.4(3) |
| $Z$ | 4 | 4 | 4 |
| reflns measured | 4737 | 24602 | 26364 |
| unique data, $R_{int}$ | 4737 | 6044, 0.0635 | 12693, 0.0360 |
| params | 196 | 408 | 838 |
| $R$ ($F$, $F^2 > 2\sigma$) | 0.0456 | 0.0388 | 0.0482 |
| $R_w$ ($F^2$, all data) | 0.1287 | 0.0890 | 0.1322 |
| GOF on $F^2$ | 1.059 | 1.091 | 1.063 |
| max, min electron density (e/Å$^3$) | 0.76, −0.48 | 0.33, −0.35 | 1.23, −0.94 |

solution changed rapidly from orange to dark red and was stirred overnight to become homogeneous. The next day, half of the solvent was removed in vacuo, and the dark red microcrystalline solid was removed by filtration, washed with a large amount of ethanol, and dried in vacuo. Crystals of the R = Me, H, and Cl derivatives suitable for X-ray diffraction were obtained by recrystallization from $CH_2Cl_2$/EtOH at room temperature.

**X-ray Crystallography.** All data were collected on a Bruker SMART CCD area diffractometer, using Mo Kα radiation ($\lambda$ = 0.71073 Å), by the $\omega$-scan method.[21] Crystal data and other experimental information are given in Table 2, with further details in the Supporting Information. Semiempirical absorption corrections were applied in all cases, on the basis of repeated and symmetry-equivalent reflections.[21] The structures were solved by direct methods and refined by full-matrix least-squares on all unique $F^2$ values.[22] Anisotropic displacement parameters were assigned to all the non-hydrogen atoms. Hydrogen atoms were placed in idealized positions and allowed to ride on their respective parent atoms. The molecule of the unsubstituted compound (R = H) lies on a crystallographic 2-fold rotation axis, passing through the Ni atom, so the asymmetric unit is half of a molecule. This structure was found to be twinned; intensities were integrated for both twin components and were retained as independent data without merging of symmetry-equivalent reflections. The ratio of the two components was refined to 0.539:0.461(2). The chloro derivative has two independent molecules in the asymmetric unit, together with a partially occupied site for a solvent dichloromethane molecule, which has been assigned half occupancy on the basis of refinement of the displacement parameters. The largest difference map features lie close to this solvent molecule, which is probably somewhat disordered. The two molecules of the complex show only minor differences in geometry.

Selected bond lengths and angles for the three complexes are reported in Table 3.

**Table 3.** Summary of Bond Lengths and Bond Angles in $[Ni(SC_6H_4R\text{-}4)_2(dppe)]^+$ (R = Me, H, or Cl; dppe = $Ph_2PCH_2CH_2PPh_2$)

| | bond length | | | bond angle | | |
|---|---|---|---|---|---|---|
| R | Ni−P | Ni−S | P−Ni−P | P−Ni−S | S−Ni−S | Ni−S−C |
| H[a] | 2.1624(7) | 2.2086(7) | 87.05(4) | 86.24(2) | 101.33(4) | 111.81(9) |
| | | | | 169.99(3) | | |
| Me | 2.1583(10) | 2.2486(9) | 86.72(4) | 84.70(3) | 98.84(3) | 99.47(11) |
| | 169.02(4) | | 2.1891(9) | 2.1933(9) | 90.77(4) | 113.16(10) |
| | | | | 169.82(4) | | |
| Cl[b] | 2.1556(11) | 2.1892(11) | 87.26(4) | 85.61(4) | 98.91(4) | 100.50(13) |
| | 2.1710(11) | 2.2389(11) | | 89.49(4) | | 111.24(13) |
| | | | | 168.36(5) | | |
| | | | | 169.72(4) | | |
| | 2.1537(11) | 2.1946(11) | 87.17(4) | 87.29(4) | 101.10(4) | 109.19(13) |
| | 2.1601(11) | 2.2244(11) | | 87.87(4) | | 111.48(14) |
| | | | | 164.35(5) | | |
| | | | | 164.27(5) | | |

[a] The molecule has crystallographic $C_2$ symmetry. [b] Two independent molecules in the asymmetric unit.

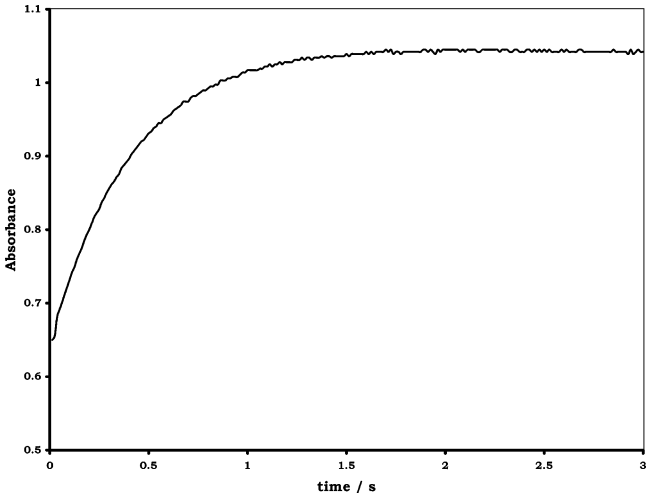


**Figure 1.** Absorbance−time curve for the reaction of $[Ni(SC_6H_4Me\text{-}4)_2(dppe)]$ (0.2 mmol dm$^{-3}$) with $[lutH]^+$ (12.5 mmol dm$^{-3}$) and lut (1.0 mmol dm$^{-3}$) in MeCN at 25.0 °C, measured at $\lambda$ = 400 nm.

**Kinetic Studies.** All kinetic studies were performed using an Applied Photophysics SX.18MV stopped-flow spectrophotometer, modified to handle air-sensitive solutions. The temperature was maintained at 25.0 ± 0.1 °C using a Grant LT D6G thermostated recirculating pump.

All solutions were prepared under an atmosphere of dinitrogen and transferred by gastight, all-glass syringes into the stopped-flow spectrophotometer. Solutions containing mixtures of lut and $[lutH]\text{-}BPh_4$ were prepared from freshly prepared stock solutions of the components, and used within 1 h.

Kinetics were studied under-pseudo first-order conditions with all reagents in a large excess (>10-fold) over the concentration of $[Ni(SC_6H_4R\text{-}4)_2(dppe)]$.[23] Under all conditions, the absorbance−time curve for the reactions is an excellent fit to a single exponential for at least 4 half-lives, indicating a first-order dependence on the concentration of complex[24] (see Figure 1). The entire curve was fitted using the Applied Photophysics computer program to obtain the observed rate constants ($k_{obs}$). The rate laws were determined by graphical analysis as described in the Results and Discussion section.

(21) *SMART* (control), *SAINT* (integration), *GEMINI* (twinning), and *SADABS* (absorption correction) software; Bruker AXS Inc.: Madison, WI, 2001.
(22) Sheldrick, G. M. *SHELXTL* version 6; Bruker AXS Inc.: Madison, WI, 2001.
(23) Espenson, J. H. *Chemical Kinetics and Reaction Mechanisms*; McGraw-Hill: New York, 1981; p 12.
(24) Wilkins, R. G. *Kinetics and Mechanisms of Reactions of Transition Metal Complexes*; VCH: Weinheim, 1991; Chapter 1.

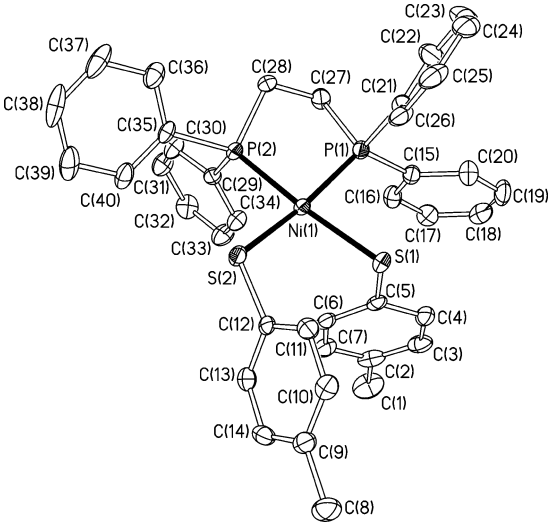


**Figure 2.** The molecular structure of $[Ni(SC_6H_4Me\text{-}4)_2(dppe)]$, with 50% probability displacement ellipsoids. H atoms are omitted for clarity.

In the kinetic studies with $[lutD]^+$, the degree of deuterium-labeling of the acid was established by $^1H$ NMR spectroscopy. We have found that even small amounts of protic impurity lead to rapid exchange even in the solid state, presumably because of the strength of this acid. Certainly, proton exchange in $[lutH]^+$ ($pK_a = 15.4$ in MeCN)[25] is more marked than for $[NHEt_3]^+$ ($pK_a = 18.46$ in MeCN).[26] Although it is impossible to entirely eliminate all protic impurities in $CD_3CN$, $^1H$ NMR spectroscopic studies show that the $[lutD]BPh_4$ used in these studies is at least 90% deuterium-labeled. In particular, the broad peak centered at $\delta$ 12.2 ppm in the $^1H$ NMR spectrum of $[lutH]^+$ is not present in the spectrum of $[lutD]^+$.

## Results and Discussion

**Structures of $[Ni(SC_6H_4R\text{-}4)_2(dppe)]$ (R = H, Me, or Cl).** The complexes, $[Ni(SC_6H_4R\text{-}4)_2(dppe)]$ (R = MeO, Me, H, Cl, or $NO_2$), were prepared by the literature methods[19] and characterized by elemental analysis and $^1H$ and $^{31}P$ NMR spectroscopies, together with the X-ray crystal structures for the R = H, Cl, and Me derivatives. The structures of the three derivatives are essentially identical, and Figure 2 shows that of $[Ni(SC_6H_4Me)_2(dppe)]$.

The structures show that the geometry about the nickel in $[Ni(SC_6H_4R\text{-}4)_2(dppe)]$ is best described as distorted square-planar. The major bond lengths and bond angles for $[Ni(SC_6H_4R\text{-}4)_2(dppe)]$ (R = H, Cl, or Me) are compared in Table 3. The Ni−P bond lengths fall in the range 2.1537(11)−2.1891(9) Å, and the Ni−S bond lengths are 2.1892(11)−2.2486(9) Å. It is worth noting that the Ni−S−C angles are somewhat variable: 111.81(9)° (R = H); 100.50(13)−111.48(14)° (R = Cl), and 99.47(11)−113.16(10)° (R = Me). These angles, as has been noted before, are normal for transition metal thiolates[27] and indicate little strain in the bound thiolates. The P−Ni−S, S−Ni−S, and P−Ni−P angles are unexceptional.

**Protonation of $[Ni(SC_6H_4R\text{-}4)_2(dppe)]$ (R = MeO, Me, H, or Cl).** The reactions between all $[Ni(SC_6H_4R\text{-}4)_2(dppe)]$ (R = MeO, Me, H, or Cl) and $[lutH]^+$ in the presence of lut, in MeCN as solvent, show all the characteristics of an equilibrium reaction. This is particularly obvious when the reaction is monitored at a single wavelength in the stopped-flow spectrophotometric studies. Thus, when the concentration of [lut] is kept constant, the absorbance change increases with increasing concentration of acid. Similarly, when the concentration of $[lutH]^+$ is kept constant, increasing the concentration of [lut] results in a decrease in the absorbance change. The kinetics of the reactions are also consistent with an equilibrium reaction.

When studied at a single wavelength using a stopped-flow spectrophotometer, the reaction between $[Ni(SC_6H_4R\text{-}4)_2(dppe)]$ (R = MeO, Me, H, or Cl) and a large excess of $[lutH]^+$ and lut (in MeCN as solvent) is typified by an absorbance−time curve which is a single exponential. The dependence on the concentrations of both $[lutH]^+$ and lut was determined graphically. A typical example is shown in Figure 3.

A plot of $k_{obs}$/[lut] against $[lutH^+]$/[lut] is a straight line with a small but finite intercept, with an associated dependence on the concentrations of $[lutH]^+$ and lut as shown in eq 1, from which the rate law shown in eq 2 is derived.

$$\frac{k_{obs}}{[lut]} = \frac{k_1^R[lutH^+]}{[lut]} + k_{-1}^R \quad (1)$$

$$\frac{-d[Ni(SC_6H_4R\text{-}4)_2(dppe)]}{dt} = \{k_1^R[lutH^+] + k_{-1}^R[lut]\}[Ni(SC_6H_4R\text{-}4)_2(dppe)] \quad (2)$$

Equation 2 is consistent with the simple equilibrium reaction[28] shown in eq 3 involving proton transfer to and from the nickel complex, where $k_1^R$ is the rate constant for proton transfer to sulfur and $k_{-1}^R$ is the rate constant for deprotonation of the coordinated thiol. The values of $k_1^R$ and $k_{-1}^R$ for R = MeO, Me, H, or Cl are summarized in Table 4.

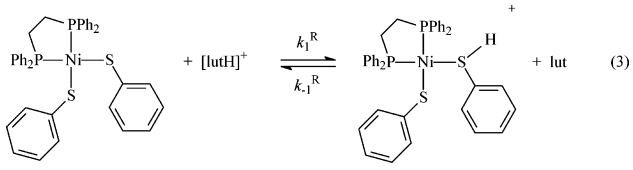


(3)

When considered in more detail both the forward (protonation) and back (deprotonation) reactions shown in eq 3 must occur by intimate mechanisms involving two distinct steps. For the protonation reaction the first step must involve approach of the acid toward the sulfur and the formation of a precursor hydrogen-bonded adduct. The protonation is completed in the second step in which intramolecular proton transfer occurs from the acid to the sulfur, within the

(25) Cauquis, G.; Deronzier, A.; Srve, D.; Vieil, E. *J. Electroanal. Chem. Interfacial Electrochem.* **1975**, *60*, 205.
(26) Izutsu, K. *Acid−Base Dissociation Constants in Dipolar Aprotic Solvents*; Blackwell Scientific: Oxford, 1990.
(27) Orpen, A. G.; Brammer, L.; Allen, F. H.; Kennard, O.; Watson, D. C.; Taylor, R. *J. Chem. Soc., Dalton Trans.* **1989**, 51.
(28) Reference 23, p 45

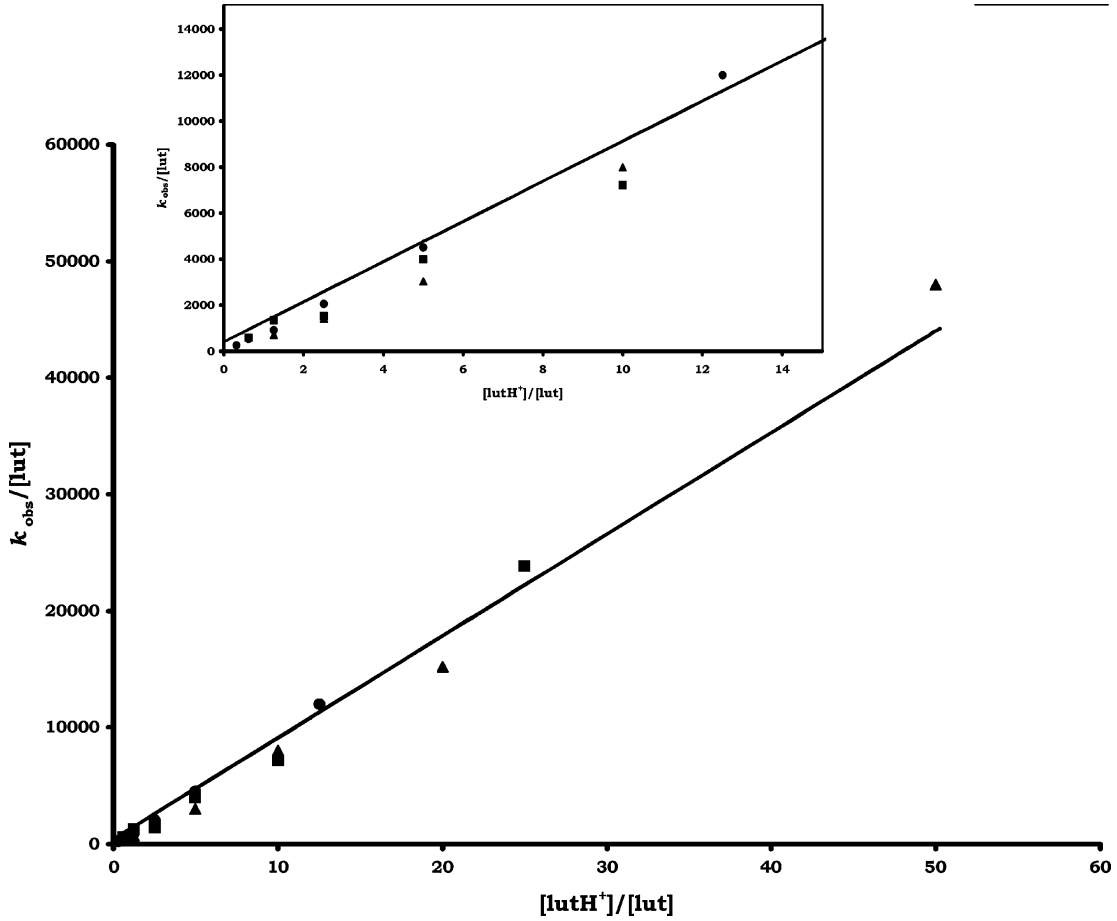


**Figure 3.** Graph of $k_{obs}$/[lut] against [lutH$^+$]/[lut] for the reaction of [Ni(SC$_6$H$_4$OMe-4)$_2$(dppe)] with [lutH]$^+$ and lut in MeCN at 25.0 °C, measured at $\lambda$ = 400 nm. The data points correspond to [lut] = 1−40 mmol dm$^{-3}$ [lutH$^+$] = 12.5 mmol dm$^{-3}$ (●); [lutH$^+$] = 25 mmol dm$^{-3}$ (■) and [lutH$^+$] = 50 mmol dm$^{-3}$ (▲). The straight line is defined by eq 2. The plot is typical of those observed for the R = Me, H, and Cl derivatives as well.

**Table 4.** Summary of Elementary Rate Constants and Activation Parameters for the Reactions of [Ni(SC$_6$H$_4$R-4)$_2$(Ph$_2$PCH$_2$CH$_2$PPh$_2$)]$^+$ with [lutH]$^+$ and lut in MeCN at 25.0 °C

| R | $k_1^R$/dm$^3$ mol$^{-1}$ s$^{-1}$ | $k_{-1}^R$/dm$^3$ mol$^{-1}$ s$^{-1}$ | $K_1^R$ | p$K_a^R$ | $\Delta H^{\ddagger}$/kcal mol$^{-1}$ | $\Delta S^{\ddagger}$/cal K$^{-1}$ mol$^{-1}$ |
|---|---|---|---|---|---|---|
| $NO_2$ | 1980[a] | 4000[b] | 0.5 | 15.1 | | |
| Cl | 360 | 300 | 1.2 | 15.5 | 23.7 | +33 |
| H | 338 | 220 | 1.5 | 15.6 | | |
| Me | 474 | 250 | 1.9 | 15.7 | 10.8 | −9.5 |
| MeO | 924 | 400 | 2.3 | 15.8 | 8.5 | −16 |

[a] $k_1^R = K_2^R k_3^R$ (R = $NO_2$). [b] $k_{-1}^R = k_{-3}^R$ (R = $NO_2$).

hydrogen-bonded adduct. The deprotonation reaction must involve analogous steps.

The simplicity of the kinetics observed with [Ni(SC$_6$H$_4$R-4)$_2$(dppe)] (R = MeO, Me, H, or Cl) means that we have no kinetic evidence for the intimate mechanism. However, for the R = $NO_2$ derivative direct kinetic evidence for the formation of a precursor adduct is obtained.

**Protonation of [Ni(SC$_6$H$_4$NO$_2$-4)$_2$(dppe)].** The reaction between [Ni(SC$_6$H$_4$NO$_2$-4)$_2$(dppe)] and an excess of [lutH]$^+$ and lut also shows all the characteristics of an equilibrium reaction. However, the kinetics of this reaction are more complicted than those observed for the other derivatives. The kinetics are illustrated in Figure 4. It is important to note that the studies with [Ni(SC$_6$H$_4$NO$_2$-4)$_2$(dppe)] were performed using the same range of [luH]$^+$ and lut concentrations as used in the studies with all the other derivatives. Consequently, the change in kinetics observed with [Ni(SC$_6$H$_4$NO$_2$-4)$_2$(dppe)] is not because of a change of reaction conditions, but rather the electronic influence of the nitro-substituent.

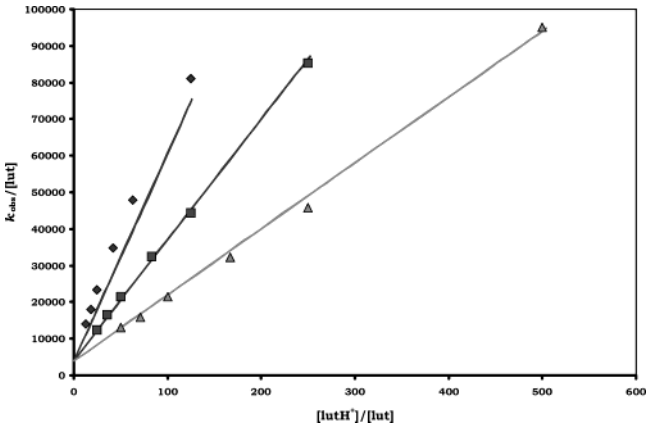


**Figure 4.** Graph of $k_{obs}$/[lut] against [lutH$^+$]/[lut] for the reaction of [Ni(SC$_6$H$_4$NO$_2$-4)$_2$(dppe)] with [lutH]$^+$ and lut in MeCN at 25.0 °C, measured at $\lambda$ = 400 nm. The data points correspond to [lut] = 0.1−1.0 mmol dm$^{-3}$ [lutH$^+$] = 12.5 mmol dm$^{-3}$ (◆); [lutH$^+$] = 25 mmol dm$^{-3}$ (■) and [lutH$^+$] = 50 mmol dm$^{-3}$ (▲). The straight lines are defined by eq 4.

For the reaction of [Ni(SC$_6$H$_4$NO$_2$-4)$_2$(dppe)], as with all the derivatives, a plot of $k_{obs}$/[lut] against [lutH$^+$]/[lut] is a straight line. The difference is that the graph is only a straight

line if the concentration of $[lutH]^+$ is kept constant. At different concentrations of acid, the gradient of the line is different, such that the higher the concentraion of $[lutH]^+$, the smaller the gradient. Analysis of the data yields the rate law shown in eq 4.

$$\frac{-d[Ni(SC_6H_4NO_2)_2(dppe)]}{dt} = \left\{\frac{1980[lutH^+]}{1 + 200[lutH^+]} + 4000[lut]\right\}[Ni(SC_6H_4NO_2\text{-}4)_2(dppe)] \quad (4)$$

Equation 4 is consistent with a mechanism involving two coupled equilibria[29] as illustrated in Figure 5. In this mechanism, the initial step in the reaction involves binding of $[lutH]^+$ to $[Ni(SC_6H_4NO_2\text{-}4)_2(dppe)]$ but without proton transfer. It seems likely that this initial binding involves hydrogen-bonding, in which the protic end of $[lutH]^+$ hydrogen-bonds to the thiolate sulfur. It is possible that, in addition to the hydrogen-bond, the binding of $[lutH]^+$ to $[Ni(SC_6H_4NO_2\text{-}4)_2(dppe)]$ could also involve aromatic $\pi-\pi$-stacking of the phenyl groups of the phosphine with the $[lutH]^+$.

The mechanism shown in Figure 5 is simply an elaboration of the single-step reaction shown in eq 3. In contrast to the other derivatives, with $[Ni(SC_6H_4NO_2\text{-}4)_2(dppe)]$ the formation of the initial hydrogen-bonded adduct is kinetically distinct from the subequent intramolecular transfer of the proton. It seems likely that the different kinetics observed with $[Ni(SC_6H_4NO_2\text{-}4)_2(dppe)]$ are because of the strongly electron-withdrawing effect of the nitro-group. The nitro-group is the most strongly electron-withdrawing 4-R-substituent employed in this series of complexes.

Consideration of the mechanism shown in Figure 5 gives the rate law shown in eq 5. The corresponding dependence of $k_{obs}$ on the concentrations of $[lutH]^+$ and lut is shown in eq 6, from which eq 7 is readily derived. Equation 7 is the basis of the graph shown in Figure 4. Comparison of eqs 4 and 5 gives the values of the elementary rate constants for the reaction between $[Ni(SC_6H_4NO_2\text{-}4)_2(dppe)]$ and $[lutH]^+$ or lut, as shown in Table 4.

$$\frac{-d[Ni(SC_6H_4NO_2)_2(dppe)]}{dt} = \frac{K_2^R k_3^R[lutH^+]}{1 + K_2^R[lutH^+]} + k_{-3}^R[lut][Ni(SC_6H_4NO_2)_2(dppe)] \quad (5)$$

$$k_{obs} = \frac{K_2^R k_3^R[lutH^+]}{1 + K_2^R[lutH^+]} + k_{-3}^R[lut] \quad (6)$$

$$\frac{k_{obs}}{[lut]} = \frac{K_2^R k_3^R[lutH^+]/[lut]}{1 + K_2^R[lutH^+]} + k_{-3}^R \quad (7)$$

Equation 5 describes the full rate law for the mechanism shown in Figure 5. However, this rate law describes the condition when the hydrogen-bonded adduct accumulates. The adduct will only attain appreciable concentrations if both $k_3^R$ and $k_{-2}^R$ are small compared to $k_2^R$. When $K_2^R[lutH^+] <$ 1, eq 7 simplifies to eq 8. Equation 8 is identical to that shown in eq 2, with $k_1^R = K_2^R k_3^R$ and $k_{-1}^R = k_{-3}^R$.

$$k_{obs} = K_2^R k_3^R[lutH^+] + k_{-3}^R[lut] \quad (8)$$

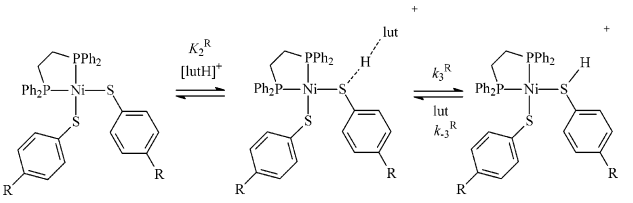


**Figure 5.** The intimate mechanism of proton transfer for the reactions of $[Ni(SC_6H_4R\text{-}4)_2(dppe)]$ (R = MeO, Me, H, Cl, or $NO_2$), as indicated by the kinetics for the R = $NO_2$ derivative.

**Basicity of Coordinated Thiolates.** From the rate constants $k_1^R$ and $k_{-1}^R$ shown in Table 4, we can calculate the protonation equilibrium constants, $K_1^R = k_1^R/k_{-1}^R$. Furthermore, since we know the p$K_a$ of $[lutH]^+$ in MeCN is 15.4,[25] the p$K_a^R$ of each $[Ni(SHC_6H_4R\text{-}4)(SC_6H_4R\text{-}4)(dppe)]^+$ can be calculated. The values are presented in Table 4. It is evident that although the p$K_a^R$ values of the complexes vary in the expected manner (i.e., lowest for R = $NO_2$ and highest for R = MeO), the value is remarkably insensitive to the 4-R-substituent. Thus, the p$K_a^R$ varies only from 15.1 (R = $NO_2$) to 15.8 (R = MeO). This variation is much smaller than anticipated with the free thiols. Athough there is no quantitative data on the strengths of 4-substituted thiols, there is information about the corresponding phenols. Thus, for 4-$MeC_6H_4OH$ (p$K_a$ = 10.2), $C_6H_5OH$ (p$K_a$ = 9.9), and 4-$O_2NC_6H_4OH$ (p$K_a$ = 7.1),[30] the acid strengths follow the expected order and cover more than 3 p$K_a$ units. It is reasonable that the corresponding thiols would show an analogous trend. It appears that, when coordinated to the nickel site, the acidities of the thiols are effectively "leveled". It is worth noting that Enemark and co-workers have observed analogous behavior in complexes of the type $[Mo(Tp)(E)(tdt)]^{n-}$ {Tp = hydrotris(3,5-dimethyl-1-pyrazolyl)borate; E = O, S, or NO; tdt = 3,4-toluenedithiolate, $n$ = 0−3}.[31] In all these complexes, the first ionization potentials are very similar, indicating that the changes in the formal oxidation state (+2 to +5) and $\pi$-effects of the E-group are neutralized by changes to the bonding of the ene−dithiolate ligand. The values of the contributing rate constants shown in Table 4 indicate that changes in the value of $k_1^R$ are mirrored by a similar change in $k_{-1}^R$.

The electronic origin of the "leveling" effect is consistent with a compensatory effect on the basicity of the sulfur atom in the complexes. In order to understand such a compensatory effect we need to consider the bonding of the thiolate and the corresponding thiol to the nickel which has been described by others.[32−34] The lone pair of electrons on the thiolate is of the correct symmetry to interact with the $t_{2g}$ d-orbitals of the metal, as shown in Figure 6. However the $t_{2g}$-orbitals in nickel are full, and a four-electron repulsion

(29) Reference 24, pp 33−37.

(30) Sykes, P. *A Guidebook to Mechanism in Organic Chemistry*, 3rd ed.; Longmans: London, 1970; p 60. p$K_a$ values are in water.

(31) Westcott, B. L.; Gruhn, N. E.; Enemark, J. H. *J. Am. Chem. Soc.* **1998**, *120*, 3382.

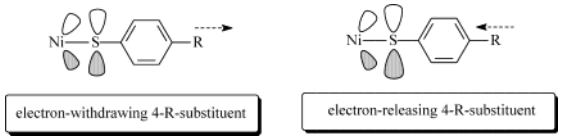


**Figure 6.** Illustration of the electronic influence of the 4-R-substituent on the interaction between the full p-orbitals on the sulfur and the full $t_2g$ d-orbitals on the nickel in complexes of the type $[Ni(SC_6H_4R\text{-}4)_2(dppe)]$.

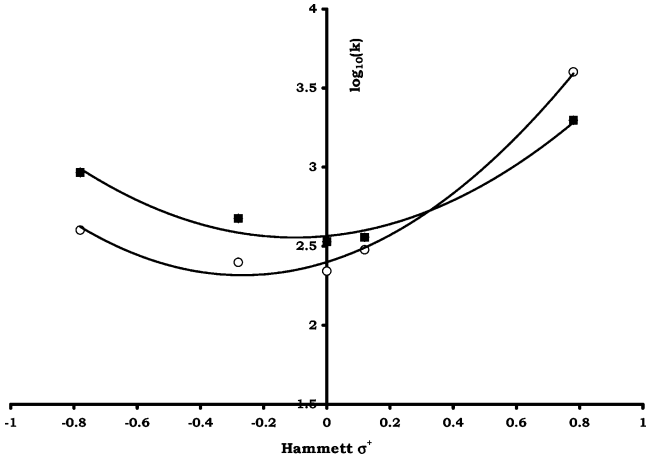


**Figure 7.** Hammett plot for the rate constants for the protonation of $[Ni(SC_6H_4R\text{-}4)_2(dppe)]$ (R = MeO, Me, H, Cl or $NO_2$) by $[lutH]^+$ ($k_1^R$, ■) and deprotonation of $[Ni(SHC_6H_4R\text{-}4)(SC_6H_4R\text{-}4)(dppe)]^+$ by lut ($k_{-1}^R$, ●). The curves are a guide to the trend of the data.

results. When the lone-pair of electrons is protonated to form the corresponding thiol, there is a reduction in the repulsion (leading to a shortening of the Ni−S bond length), and a weakening of the $\sigma$-donation since thiol is a neutral ligand but thiolate is anionic (leading to a lengthening of the Ni−S bond length). Thus, electron-donating 4-R-substituents would be expected to increase the electron density of the sulfur in thiolates, but this would be tempered by the added repulsion with the $t_{2g}$ orbitals on nickel. In contrast, electron-withdrawing 4-R-substituents diminish the electron density at the sulfur but also permit closer interaction between the nickel and sulfur. These electronic effects result in an effective leveling of the $pK_a^R$ of the coordinated thiol through a modulation of the degree of covalency of the Ni−S bond.

**Rates of Proton Transfer.** The rates of proton transfer are affected by the 4-R-substituent (Table 4). The influence of the 4-R-substituent on $k_1^R$ and $k_{-1}^R$ is illustrated in the Hammett plot shown in Figure 7. We have used the Hammett $\sigma^+$ parameter for the correlation, since this parameter allows for conjugation between the 4-R-substituent and the reaction site (sulfur). Previous studies[35] have indicated that this parameter is more appropriate in the reactions of ligands on transition metal complexes than the Hammett $\sigma$ parameter. Interpretation of the effect that the 4-R-substituent has on the rate of proton transfer is complicated by two features. First, the measured rate constants ($k_1^R$ and $k_{-1}^R$) are composite values comprising the elementary reactions of (i) binding of the acid to form the hydrogen-bonded species followed by (ii) intramolecular proton transfer. Second, the Hammett $\sigma^+$ parameter reflects only electronic resonance effects but neglects electronic inductive effects. Recent theoretical calculations[36] have used the Natural Bond Order package to calculate the electron density on the sulfur atoms of thiols and disulfides. However, the values of $k_1^R$ and $k_{-1}^R$ do not correlate well with these calculated values of the electron density on the sulfur.

It is evident that the effect the various 4-R-substituents have on the rates of proton transfer is not so simplistic as the modulation of the electron density (basicity) of the sulfur site. As we have seen above, the basicity of the site is relatively insensitive to the substituent. As the kinetics of the reaction between $[Ni(SC_6H_4NO_2\text{-}4)_2(dppe)]$ and $[lutH]^+$ reveal, the mechanism for the protonation of all $[Ni(SC_6H_4R\text{-}4)_2(dppe)]$ consists of two steps: the formation of a hydrogen-bonded adduct followed by intramolecular proton transfer. Consequently, the values of $k_1^R$ and $k_{-1}^R$ reflect the net effect of the 4-R-substituent on both the adduct formation and intramolecular proton transfer. It seems reasonable that the binding constant for the formation of the hydrogen-bonded adduct would depend on the electron density at the sulfur and hence correlate with the $pK_a^R$. As discussed above, the $pK_a^R$ of $[Ni(SHC_6H_4R\text{-}4)(SC_6H_4R\text{-}4)(dppe)]^+$ is rather insensitive to the nature of the 4-R-substituent, and hence, it seems likely that Figure 7 reflects the effect that the 4-R-substituent has on the rate of intramolecular proton transfer. This proposal is justified in the succeeding paper, where studies on $[Ni(SC_6H_4R\text{-}4)(triphos)]^+$ show that the rate of intramolecular proton transfer with these complexes correlates with the electron density on the sulfur.[16]

It is evident from Figure 7 that the same factors which facilitate proton transfer to the sulfur ($k_1^R$) also facilitate proton transfer from the coordinated thiol ($k_{-1}^R$). How both electron-releasing and electron-withdrawing 4-R-substituents facilitate proton transfer to and from sulfur is rationalized in terms of the bonding description shown in Figure 6.

Proton transfer to thiolate sulfur is facilitated by electron-donating substituents because of the increased electron-density on the sulfur (reflected in $pK_a^R$). Effectively, this is a ground state destabilizing effect. As discussed above, electron-withdrawing 4-R-substituents will diminish the unfavorable interaction between the full p-orbitals on the sulfur and the full $t_{2g}$-orbitals on the nickel.[37] Protonation of a thiolate ligand has a similar effect on the Ni−S orbital interaction. Consequently, electron-withdrawing substituents facilitate the protonation reaction by effectively making the nickel−thiolate orbital interaction more like that of the nickel−thiol. Effectively, this is a transition state stabilization effect.

We consider now the rate of deprotonation of the thiol complex. Proton transfer from thiol sulfur is facilitated by

(32) Grapperhaus, C. A.; Pothrovic, S.; Mashata, M. S. *Inorg. Chem.* **2002**, *41*, 4309.
(33) Ashby, M. T.; Enemark, J. H.; Lichtenberger, D. L. *Inorg. Chem.* **1988**, *27*, 191.
(34) Grapperhaus, C. A.; Patra, A. K.; Mashata, M. S. *Inorg. Chem.* **2002**, *41*, 1039.
(35) Hussain, W.; Leigh, G. J.; Mohd Ali, H.; Pickett, C. J.; Rankin, D. A. *J. Chem. Soc., Dalton Trans.* **1984**, 1703.
(36) Sengar, R. S.; Nemykin, V. N.; Basu, P. *New. J. Chem.* **2003**, *7*, 1115.
(37) Sellmann, D.; Sutter, J. *Acc. Chem. Res.* **1997**, *30*, 460 and references therein.

electron-withdrawing substituents because of the increased acidity of the coordinated thiol (i.e., ground state destabilization). In complexes where the coordinated thiol contains an electron-donating 4-R-substituent, the unfavorable orbital interactions in the nickel−sulfur bond are enhanced as they are in the thiolate product (i.e., transition state stabilization).

**Temperature Dependence of the Reactions.** The effect of temperature on the reactions of $[Ni(SC_6H_4R\text{-}4)_2(dppe)]$ (R = MeO or $NO_2$) with $[lutH]^+$ have been studied.[38] The activation parameters determined from analysis of the data are characterized by an effectively constant $\Delta G^{\ddagger} = 13.6 \pm 0.3$ kcal mol$^{-1}$. However, the contributing values of $\Delta H^{\ddagger}$ and $\Delta S^{\ddagger}$ vary significantly, as shown in Table 4. Thus, as the 4-R-substituent becomes more electron-withdrawing, $\Delta H^{\ddagger}$ becomes larger and $\Delta S^{\ddagger}$ becomes more positive (R = MeO, $\Delta H^{\ddagger} = 8.5$ kcal mol$^{-1}$, $\Delta S^{\ddagger} = -16$ cal K$^{-1}$ mol$^{-1}$; R = Me, $\Delta H^{\ddagger} = 10.8$ kcal mol$^{-1}$, $\Delta S^{\ddagger} = -9.5$ cal K$^{-1}$ mol$^{-1}$; R = Cl, $\Delta H^{\ddagger} = 23.7$ kcal mol$^{-1}$, $\Delta S^{\ddagger} = +33$ cal K$^{-1}$ mol$^{-1}$). The values of $\Delta H^{\ddagger}$ and $\Delta S^{\ddagger}$ give further insight into the intimate mechanism of proton transfer in these complexes. The trend observed in the values of $\Delta H^{\ddagger}$ and $\Delta S^{\ddagger}$ is consistent with a description of the transition state in which the position of the proton between $[lutH]^+$ and the thiolate sulfur during the proton transfer depends on the nature of the 4-R-substituent.

When the 4-R-substituent is strongly electron-releasing (e.g., R = MeO) the sulfur is sufficiently basic that, upon approach of the $[lutH]^+$, the proton is attracted (and hence is close) to the sulfur. The subsequent transfer of the proton to the sulfur thus involves only proton transfer over a short distance. We propose that $\Delta H^{\ddagger}$ reflects the distance the proton has to transfer. The negative value of $\Delta S^{\ddagger}$ reflects a tight, productlike transition state. For electron-withdrawing 4-R-substituents (e.g., R = Cl), approach of $[lutH]^+$ toward the sulfur results in a hydrogen-bonded adduct in which the proton is still predominantly associated with the nitrogen of lut. In order to complete the transfer, the proton has to move an appreciable distance ($\Delta H^{\ddagger}$ is large), and the transition state is more reactant-like ($\Delta S^{\ddagger}$ is positive).

**Isotope Effects.** We have studied the effect on the rate of using $[lutD]^+$ for selected complexes. The kinetics for the reactions of $[Ni(SC_6H_4Me\text{-}4)_2(dppe)]$ or $[Ni(SC_6H_4Cl\text{-}4)_2(dppe)]$ with $[lutD]^+$ in the presence of lut show that the reaction is associated with a negligible kinetic isotope effect. The use of the aprotic solvent MeCN means that the isotopic label is not lost in rapid exchange with the solvent, and hence, the small kinetic isotope effect ($k_1^H/k_1^D = 1.0 \pm 0.1$) is unambiguously associated with the transfer of a proton.

Previous studies[39] have shown that weak kinetic isotope effects are observed because of (i) limiting asymmetry in the transition state; (ii) heavy atom participation in the reaction coordinate resulting in an increase in isotope-sensitive zero point energy of the transition state; or (iii) bending modes orthogonal to the reaction coordinate which add additional isotope zero point energy to the transition state. We are not able to distinguish which of these aspects is dominant in the reactions of $[Ni(SC_6H_4R\text{-}4)_2(dppe)]$ with $[lutH]^+$.

Negligible kinetic isotope effects have been observed in other systems where, similar to that presented herein, the reaction only involves the transfer of a hydrogen, or proton. Most notably the addition of dihydrogen[40] to *trans*-$[IrCl(CO)(PPh_3)_2]$ to form $[Ir(H)_2Cl(CO)(PPh_3)_2]$ has an isotope effect $k^H/k^D = 1.09$ at 25.0 °C. This small value has been attributed to the compensatory effect of an unusually large mass and moment of inertia term (arising from translational and rotational partition functions), a moderate inverse excitation term (vibrational partition functions), and a substantial inverse zero point energy factor. In the proton transfer reactions of 2,4-dinitrophenol with $NEt_3$ or piperidine, there is no kinetic isotope effect; this has been attributed to the lack of hydrogen bonding between the phenol and these strong bases. In contrast, the reaction with the weaker base, pyridine, where hydrogen bonding does occur, is associated with a significant isotope effect.[41]

## Summary

In this paper we have described the synthesis, characterization, and protonation reactions of $[Ni(SC_6H_4R\text{-}4)_2(dppe)]$ (R = MeO, Me, H, Cl, or $NO_2$). The kinetics of the reaction between $[Ni(SC_6H_4NO_2\text{-}4)_2(dppe)]$ and $[lutH]^+$ indicate a mechanism in which initial rapid formation of a hydrogen-bonded adduct occurs prior to the intramolecular transfer of the proton within the hydrogen-bonded adduct. Analysis of the kinetics allows determination of the rate constants and equilibrium contants associated with each of the steps. To date, intramolecular proton transfer reactions have been little studied, despite the fact that such reactions play crucial roles in enzymes where the access of protons to the active site needs to be limited.[42] Unfortunately, only with the nitro-derivative is the intramolecular proton transfer step kinetically distinguishable from the formation of the precursor hydrogen-bonded adduct. In the succeeding paper, we explore intramolecular proton transfer reactions in nickel thiolate complexes in more detail. In particular, we will show that the reactions of all the derivatives of $[Ni(SC_6H_4R\text{-}4)(triphos)]^+$ (R = MeO, Me, H, Cl, or $NO_2$) with $[lutH]^+$ exhibit kinetics which allow determination of the rate constants for intramolecular proton transfer within the hydrogen-bonded precursor, providing a complete kinetic description of the factors affecting the rates of the largely unexplored intramolecular proton transfer reactions.

**Supporting Information Available:** X-ray crystallographic files in CIF format for the three crystal structures and kinetic data for the reactions of $[Ni(SC_6H_4R\text{-}4)_2(dppe)]$ (R = MeO, Me, H, Cl, or $NO_2$). This material is available free of charge via the Internet at http://pubs.acs.org.

IC030322E

(38) Reference 23, pp 116−122.
(39) Ozaki, A. *Isotopic Studies in Heterogeneous Catalysis*; Academic Press: New York, 1976; pp 172−178.
(40) Zhou, P.; Vitale, A. A.; San Filippo, J., Jr.; Saunders, W. H., Jr. *J. Am. Chem. Soc.* **1985**, *107*, 8049.
(41) Bell, R. P.; Crooks, J. E. *J. Chem. Soc.* **1962**, 3513.
(42) Stubbe, J.; Nocera, D. G.; Yee, C. S.; Chang, M. C. Y. *Chem. Rev.* **2003**, *103*, 2167 and refs therein.